

Radium Sorption to Iron (hydr)oxides, Pyrite, and Montmorillonite: Implications for Mobility

Author, please respond to the following questions:

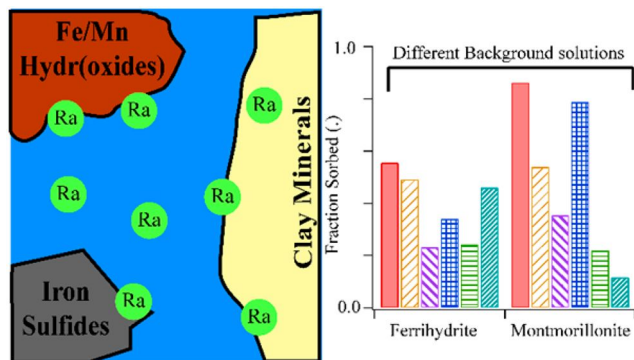
Author: Please examine Figure 3 to verify that the y-axis should read “Fraction Sorbed (.)” 7

Michael A. **Chen** ■ and Benjamin D. **Kocar** * ■ ■

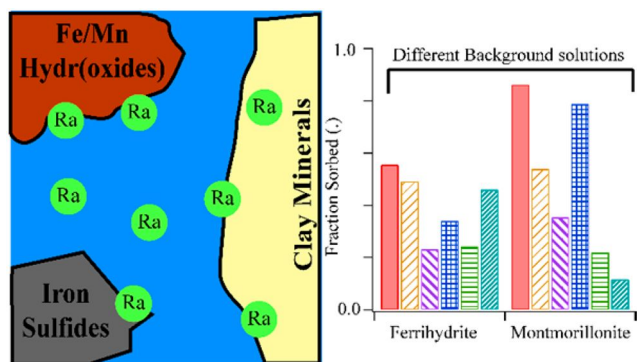
Dept. Department of Civil and Environmental Engineering, Massachusetts Institute of Technology, 77
Massachusetts Avenue, Cambridge, Massachusetts 02142, **United States**

*Corresponding Author Phone: Benjamin 617-324-7746 D. Kocar; e-mail: kocar@mit.edu, 15 Vassar Street, Building 48-323 (B.D.K. Department of Civil and Environmental Engineering, Massachusetts Institute of Technology, Cambridge, MA 02139). kocar@mit.edu - 617-324-7746

Radium (Ra) is a radioactive element commonly found within soils, sediments, and natural waters. Elevated Ra activities arising through natural and anthropogenic processes pose a threat to groundwater resources and human health, and Ra isotope ratios are used to decipher groundwater movement, estimate submarine discharge flux, and fingerprint contamination associated with hydraulic fracturing operations. Although adsorption to metal (hydr)oxides and certain clay minerals is well established as a dominant mechanism controlling Ra transport and retention, the extent of Ra sorption to other minerals and under variable environmental conditions (e.g., pH and salinity) is limited. Accordingly, we present results of sorption studies and surface complexation modeling (SCM) of Ra to ferrihydrite, goethite, montmorillonite, and pyrite, for a range of pH values and common background cations. Ra sorption to all substrates is observed under geochemical conditions considered, but varies according to mineral, solution pH and specific competing cations. Literature derived SCMs for Ra sorption were fitted to match either sorption impacts due to pH or different background cations, but were not able to predict the impacts of different geochemical conditions. Despite this, the use of SCMs provided a more mechanistic understanding of Ra sorption as compared to commonly used distribution coefficients.



Abstract Graphic



TOC Graphic

SI File: es7b05443_si_001.pdf

Introduction

Chronic ingestion and inhalation of radioactive materials, including radium (Ra) and radon (Rn), represents an ongoing threat to human health worldwide.¹ Of these, Ra is ubiquitous in soils, aquifers, and natural waters owing to the radioactive decay of primordial ²³⁵U, ²³⁸U, and ²³²Th, and often accounts for the dominant fraction of total radiation found in groundwater. All isotopes of Ra are unstable, and four (²²³Ra, ²²⁴Ra, ²²⁶Ra, and ²²⁸Ra) possess half-lives sufficient to persist within environmental systems and present a risk for human exposure (11.4 days, 3.6 days, 1600 years, and 5.75 years, respectively). Moreover, ²²⁶Ra is the parent radionuclide of ²²²Rn; chronic inhalation of ²²²Rn increases risk of lung cancer.² Hence, geochemical controls on Ra mobility are directly tied to the mobility and accumulation of Rn within soil-sedimentary systems.

Several geochemical processes impart overarching controls on Ra within soils and aquifers. Alpha-recoil, the ejection of daughter radionuclides from soil and sedimentary minerals into adjacent porewater, is a primary process sourcing Ra to groundwater. Ongoing alpha recoil progressively elevates porewater Ra activities until hydrologic flushing removes the equilibrating solution, or Ra achieves secular equilibrium with its parent and daughter nuclides. Most aquifer systems contain low (e.g., U, Th, < 5 mg/kg) but adequate parent radionuclide and sufficiently favorable hydrological conditions to facilitate delivery of measurable Ra to solution.³ In a recent USGS study, 3% of groundwater samples ($n = 1270$) within 7 of 15 principal **USU.S.** aquifers exceeded the USEPA limit for total Ra of 0.185 Bq/L.⁴ Further, high levels of Ra are often present with deeper formations, particularly shales, where low groundwater flux yield potentially hazardous activities (0.102–343 Bq/L).⁵ These naturally elevated Ra bearing formations are prevalent in some parts of the **USU.S.** (PA, WY, TX).⁶ Anthropogenic activities, including uranium mining and hydraulic fracturing, can redistribute Ra and other constituents of naturally occurring radioactive materials (NORM), posing potential hazards to populations nearby affected soils, surface waters, and aquifers.

Under environmental conditions, Ra is not redox active, and its solution speciation is dominated by free $\text{Ra}^{2+}_{(\text{aq})}$ across a wide range of chemical conditions (e.g., pH and salinity). Weak complexes with carbonate, sulfate, and chloride are observed, but these solution species are only important at extremely acidic or basic pH values and when ligand activities exceed environmental relevance.⁷ The Ra^{2+} ion participates in several geochemical reactions that constrain (or enhance) its solubility, resulting in **non-conservative** transport in aquifers. Sorption is generally regarded as the dominant process controlling Ra solubility of in many soil and groundwater systems.^{8,9} Alternatively, **co-precipitation** of Ra with Ba and Sr sulfates can rapidly remove Ra from solution, but this depends on elevated (~1 mM) levels of Ba, Sr, and SO_4^{2-} to proceed, and does not completely scavenge Ra from solution.¹ Concurrently with these physical and chemical processes, Ra isotopes undergo radioactive decay. While ²²⁶Ra and ²²⁸Ra have long enough half-lives to persist in groundwater aquifers, the fast decay rate of ²²⁴Ra and ²²³Ra generally result in minimal activities in natural waters.

Soil and sedimentary minerals known to sorb appreciable quantities of Ra include metal (hydr)oxides and 2:1 clays with an exchangeable interlayer.^{10–14} The work studying these minerals have resulted in K_d values for Ra sorption to different soil and aquifer materials in NaCl or NaClO₄ background solutions (**Table S3 of the Supporting Information, SI**), but are of limited use for deciphering the impact shifts in geochemical condition (ie. pH, salinity, background cation concentrations), and typically do not address differences between minerals for a specific geochemical condition. It is also well established that Ra solubility is enhanced with increased ionic strength, but there are only a few studies

that examine the impact of different, specific cations on Ra sorption to metal oxide minerals.^{13–16} These studies have shown that multivalent ions have a competitive effect on Ra sorption, even when at limited (~mM) concentrations, but there has not been a systematic accounting of each ion's impact, particularly for common groundwater elements such as K and Mg. Additionally, the impact of these cations on Ra sorption to clay minerals, which typically contain exchangeable cations in inter-layer/interlayer sites, has not been quantified. There is also a paucity of data regarding Ra adsorption to redox-sensitive minerals found under suboxic or reducing conditions. These solids, including metal sulfides such as pyrite, may be particularly important within soil and aquifer systems derived from shale, and also within marine sediments—including those which intercept submarine groundwater discharge that carry naturally occurring Ra.

Improved knowledge of Ra sorption to common soil and sedimentary solids and with different background solutions is required to decipher Ra mobility and predict total activities within natural waters. This understanding can also aid in interpreting Ra isotopic ratios used to trace sources of Ra and understand groundwater movement. The objectives of this study were to therefore: (1) examine and compare low-activity Ra adsorption to ferrihydrite, goethite, and Na-montmorillonite—minerals known or inferred to control Ra transport over a range of solution conditions found in soils and aquifers—and pyrite, a mineral commonly found within reduced and anoxic soils and sediments, (2) examine the impact of individual and mixtures of cations on Ra sorption, and (3) use surface complexation modeling (SCM) as a quantitative means for comparing the extent of Ra adsorption between different minerals and geochemical conditions, and evaluate their accuracy for predicting Ra sorption under different solution conditions.

Materials and Methods

Dissolved ²²⁶Ra stock in 3% HCl was provided by the MIT Environmental, Health, and Safety office and used for all experiments. A ferrihydrite slurry and goethite powder were prepared using standard methods and added to the experiments.¹⁷ Powdered calcium montmorillonite STX-1b was ordered from The Clay Minerals Society (clays.org), re-equilibrated with sodium chloride to allow for closer comparisons to previous studies of Ra sorption to Na-montmorillonites, and then cleaned of carbonates using standardized techniques.¹⁶ Cubic pyrite was ordered from Ward's Science (www.wardsci.com), ground using mortar and pestle, passed through sieves to select for 45–250- μ m particles, and transferred to an anoxic glove bag/glovebag (H₂: 2% , N₂: 98%, O₂: < 1 ppm). It was then washed in 6 N HCl overnight to dissolve any oxidized coatings, rinsed with deoxygenated DI water three times to remove residual acid, and dried anoxically at room temperature. The composition of pyrite, ferrihydrite, and goethite was confirmed using XRD, and surface area was measured for all minerals using BET (Table S1). Further information regarding mineral preparation is found in the supporting information SI.

All experiments were conducted using serum vials (200 mL) filled with 100 mL of background solution, 30 mg of a single mineral (except for the case of pyrite, where 40 mg was used), and 3–320 Bq of ²²⁶Ra stock. Isotherms were performed at pH 3, 5, 7, or 9 \pm 0.05 using 10 mM NaCl stock as the background solution. The impact of different background cations on Ra adsorption to ferrihydrite, goethite, pyrite, and sodium montmorillonite was elucidated at pH 7 \pm 0.05 using 10 mM CaCl₂, MgCl₂, KCl, SrCl₂, or a 10 meqmequiv/L ionic strength artificial groundwater (AGW) (Table S2). The impact of increasing ionic strength on Ra sorption to these minerals was examined with a pH 7 \pm 0.05, 100 meqmequiv/L artificial brackish water (ABW) and 800 meqmequiv/L artificial seawater (ASW) (Table S2). Experiments using pyrite were performed in a sub-oxiesuboxic (<1 ppm of O₂) glove bag/glovebag, and all solutions were purged with N₂ prior to placement in the anoxic chamber. For all experiments, an auto-titrator was used to assist pH adjustment, and bottles were sealed with a thick butyl stopper. Bottles were shaken for 24 hours to allow sufficient time for sorption equilibrium.¹⁴ A kinetic study of Ra adsorption to montmorillonite confirmed 24 hours is sufficient to achieve equilibrium (SI). pH was readjusted after equilibration if necessary; details on this process are in the supporting information SI. Acid (HCl) and base (NaOH) volume additions did not exceed 5% of the original solution-slurry volume. Once re-titration and re-equilibration were complete, samples were filtered using 0.22- μ m PES filters, which did not sorb significant quantities of Ra. Experimental error was quantified by measuring the standard deviation of triplicates for each data point.

Analytical Techniques

Solutions of Ra were quantified using scintillation counting. Up to 10 mL of sample were mixed with 10 mL of Ultima Gold XR (Perkin Elmer/PerkinElmer) and sealed for 30 days to allow ²²⁶Ra to reach secular equilibrium with its daughter products.¹⁸ The equilibrated samples were then counted using a Beckman Coulter LS 6500 scintillation counter, and the resulting counts were compared to a calibration curve of similarly prepared ²²⁶Ra standards (see SI) to determine solution activities.

Surface Complexation Modeling

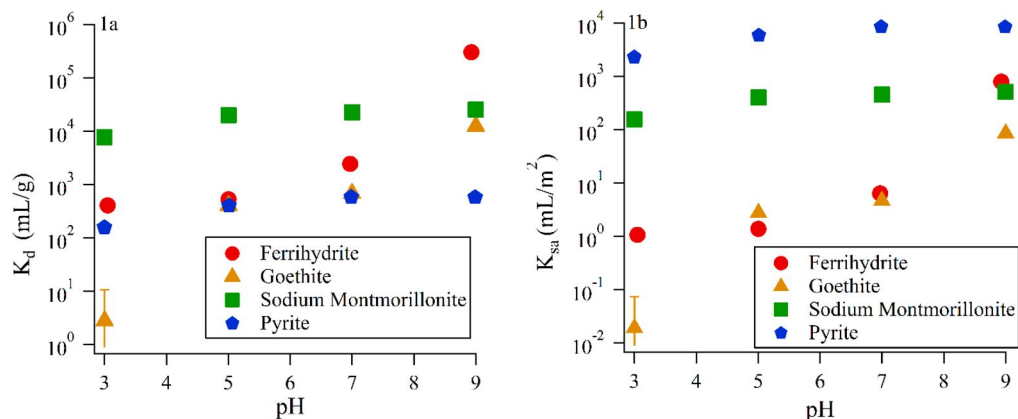
Ra interaction with mineral surfaces was modeled through mineral specific surface complexation models implemented in PHREEQC.¹⁹ The IPHREEQC COM module was used in conjunction with a python script to easily enable multiple realizations of the SCM for fitting.²⁰ The naturally low levels of Ra in the environment combined with the significant radiotoxicity of Ra have hindered the development of spectroscopically informed models of Ra-specific SCMs. Thus, in all cases, relatively simple SCMs that have already been established in the literature are used, except for pyrite, where fitting of any previously published models did not produce reasonable fits.^{21,22} For the iron (hydr)oxides, a double diffuse layer model is used following work following Dzombak and Morel's work.^{21,23} In the case of sodium montmorillonite, a ~~non-electrostatic~~ nonelectrostatic model using both protonated surface sites and cation exchange sites following Bradbury and Baeyens' work was used, namely, the 2 site protolysis ~~non-electrostatic~~ nonelectrostatic surface complexation model and cation exchange model (2SPNE SC/CE).²² For clarity, when discussing SCM, we also mean to include the 2SPNE SC/CE model, even though it contains both SCM and ion exchange. Ra surface complexes were derived from group II cation SCM reactions published by previous studies, and then fit experimental data. These models were supplemented with adsorption reactions for competing ions, whose constants were directly taken from literature values or derived from linear free energy relationships posed in previous studies.^{21,23-29} Model fits to data were achieved through varying the thermodynamic constant for each Ra (ad)sorption reaction. Fitting was performed on isotherm data and data from experiments testing the effects of competing cations on Ra sorption; thermodynamic constants developed for each set of experiments were then compared. Details for fitting SCMs, discussion of the choices of SCMs, and the different pyrite SCMs tried are found in the ~~supporting information~~ SI.

Results and Discussion

Sorption ~~isotherms~~ Isotherms

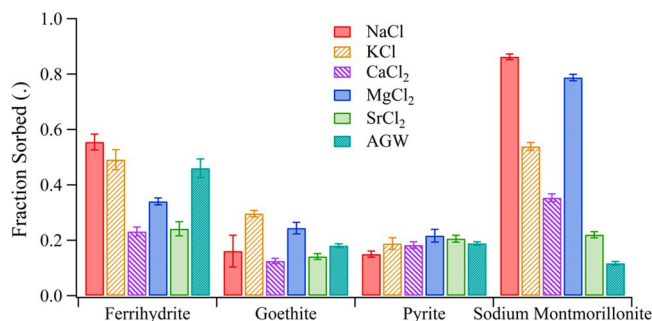
All isotherms using 10 mM NaCl were linear in the range of activities considered (~~figure~~Figure S1), and thus each were fitted to a line using a least-squares method, whose slope corresponds to the (mass normalized) K_d for that isotherm (~~figure~~Figure 1 a). Sorption to both iron (hydr)oxides show a strong dependence on pH, with ferrihydrite showing greater sorption across all pH values compared to goethite, and the extent of sorption increasing with increasing pH for both iron (hydr)oxides. Differences in the extent of Ra sorption between goethite and ferrihydrite may be explained by disparate surface areas, with ferrihydrite having nearly twice the surface area of goethite. Fitted K_d values were normalized by the measured surface area to derive a K_{sa} (~~figure~~Figure 1 b), showing that at circumneutral pH, goethite and ferrihydrite have close K_{sa} values, however, at more extreme values (pH = 3 and pH = 9) ferrihydrite demonstrates an appreciably larger extent of sorption compared to goethite. Hence, differences in surface area only partially explain the discrepancy in Ra sorption between these minerals; differences in mineral (electro)chemical surface environment likely play an important role. For example, the different Fe coordinations (tetrahedral and octahedral) found in ferrihydrite could result in larger surface site affinity for Ra^{2+} as compared to the single octahedral coordination environment of Fe atoms in goethite.^{30,31} Two studies have reported isotherm data for Ra sorption to ferrihydrite.^{14,15} The K_d found in our study is larger than found in those studies by at least a factor of 2 (SI for values and comparison), but was also performed at lower background ionic strength (here, 10 mM NaCl, others, 100–500 mM) and higher mineral surface area (here, 382.9 m²/g, others, ~250 m²/g). K_{sa} values were fairly close to those reported in other studies, with higher background solution ionic strength matching with smaller K_{sa} , consistent with previously reported results that increasing ionic strength decreased Ra sorption to iron (hydr)oxides.¹⁵

Figure 1. K_d (left, ~~figure~~1aa) and K_{sa} (right, ~~figure~~1bb) values developed from linear fitting of experimental isotherm data.



Results for mass normalized (K_d) and surface area normalized (K_{sa}) sorption of Ra onto sodium montmorillonite are plotted in [Figures 1 and 2](#). With the exception of ferrihydrite at pH 9, the total extent of sorption to montmorillonite is larger than iron (hydr)oxides over all pH values regardless of normalization. Also, a comparatively weaker pH dependence is observed for montmorillonite sorption. This result implies that the dominant mechanism controlling montmorillonite sorption is not complexation with pH dependent surface (edge) functional groups, but rather exchange of Ra with clay interlayer cations. Unlike with the iron (hydr)oxides, the K_d and K_{sa} values were larger by nearly an order of magnitude compared to previous studies, in spite of similar background solution composition. ^{11,16} Those used a high solid-solution ratio (3000–50000–50000 mg solid/L) but resulted in less sorption compared to the sorption results found here, which used only a 300 mg/L solid-solution ratio. The CEC of the clay used here (84.4 meqmequiv/100g, clay minerals society) falls within the range of those other studies (76.4–120 meqmequiv/100g), as does the surface area (50.2 m²/g, [table S1](#) compared to 31.82–97.42 m²/g from clay minerals society). ²⁵ Given the similar experimental conditions, one would expect that K_d values would also be similar. This discrepancy may be explained by mineralogical differences that are not readily captured by these common sorption parameters, as this study and the previous studies each used a different type of montmorillonite (here, STx-1b, Tamamura, SWy-2, Ames, SAZ-1). For example, structural variation, including the extent of isomorphous substitution, will drive differences in Ra affinity for surface and interlayer sites. ²⁵

Figure 2. Impact of competing cations on Ra sorption at similar ionic strengths (pH = 7).



Ra sorption to pyrite was low, but appreciable all pH values, and weak dependence on pH ([figure 1](#)), with similar sorption to ferrihydrite at acidic pH values. Unexpectedly, surface area normalized sorption isotherms show that pyrite has the largest sorption of all the minerals considered here ([figure 2](#)). There is very little existing data examining the sorption of Ra to any reduced iron solid. A previous study demonstrated that strontium (Sr), which possesses similar geochemical characteristics as Ra, did not sorb extensively to pyrite; ³² In contrast, a variety of experimental and spectroscopic techniques have been used to study redox active metal ions sorption to the pyrite surface, which often includes redox reactions between the metal ion and pyrite surface groups. ^{32–37} The results of these studies imply that redox active metal ions or trace quantities of dissolved oxygen in solutions with Ra may alter the

pyrite surface, consequentially diminishing or enhancing Ra sorption depending on the iron (hydr)oxide phase formed. However, we find no evidence of oxic pyrite alteration in our experiments, and use exceedingly low Ra concentrations (0.06–31 nmoles per experiment) which preclude using analytical methods for examining the coordination environment of adsorbed Ra. The difference in reported Sr sorption and Ra sorption may instead be driven by natural pyrite impurities that may impact Ra sorption affinity for the pyrite surface. Authigenic pyrite found in natural shales and estuarine settings may show enhanced sorption, as they may have larger effective surface area than the crushed pyrite used here.

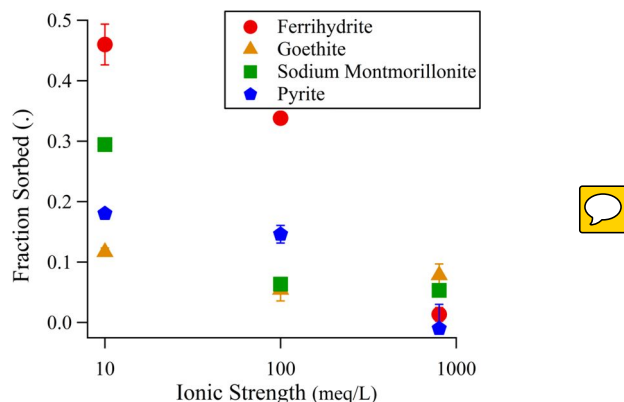
Background-cation controls Cation Controls on Ra sorption Sorption

Experiments using different background electrolytes, but with similar ionic strength, initial concentration of Ra (60–70 Bq total activity) and pH (7.0) illustrate notable deviations from Ra adsorption trends observed using NaCl (Figure 2). Sodium montmorillonite shows large changes in Ra retention in the presence of different competing cations. Notably, the use of the 10 mM ionic strength AGW altered trends originally observed for Ra isotherms using a 10 mM NaCl background, with ferrihydrite having a larger sorption extent compared to the montmorillonite. This is likely a result of background cation competition for interlayer exchange sites in the clay, which are absent in the iron (hydr)oxides. Less Ra sorption was observed in the presence of divalent cations compared to monovalent cations, as did heavier ions, with Sr-bearing solutions resulting in minimal Ra sorption to all minerals. Ra sorption to pyrite showed little sensitivity to cation type. Overall, less adsorption of Ra to all substrates is observed in experiments in which AGW is used as compared to a single ion alone. This is the most drastic for sodium montmorillonite, where there is a clear synergistic effect between the cations that results in less Ra sorption in the mixed background solution than is observed for any single cation background solutions. The presence of this synergistic effect is less clear for the iron minerals. Further study of these potential synergistic impacts is necessary to predict sorption of Ra to minerals within natural systems.

The impact of the different cations on Ra sorption also varied depending the mineral. For example, goethite showed maximal Ra sorption with K^+ as the background cation, yet the other minerals clearly showed maximal sorption with Na^+ as the background. This defies the usual trend of heavier elements in the same group sorbing more than the lighter elements due to the increase of atomic size and subsequent increase in sorption site availability. Previous studies of Ra have also addressed the role of competing background cations; a ratio of 1:1 Ca:Na in the background solution was shown to decrease Ra sorption to ferrihydrite by ~20%, while even ratios of 1:100 Ba:Na in the background were able to decrease sorption by 10% or more.¹⁴ This is consistent with our artificial groundwater results for Ra sorption to ferrihydrite, which had 1:10 ratio of Ca:Na (alongside other competing ions). These results demonstrate that sorption data from experiments using background solutions dominated by a single monovalent cation such as sodium may overestimate the extent of Ra sorption compared to natural solutions harboring a diversity of mono and multi-valent multivalent cations, and shifts in groundwater ion composition (i.e., driven by mixing of different source waters) could alter Ra sorption to aquifer materials. This is particularly relevant for hydraulic fracturing systems where injected groundwaters tend to have a different ionic composition compared to the natural formation brine.

Experiments to examine the influence of increasing ionic strength were also performed, using the same ratio of cations used in the AGW (table Table S2), but with increasing total ionic strength (figure Figure 3). Specifically, “brackish” (100 meqmequiv/L) and “seawater” (800 meqmequiv/L) ionic strengths were used (pH 7.0). As with experiments using different electrolyte compositions, the greatest decrease in Ra sorption occurred in treatments using sodium montmorillonite; sorption decreased 80 percent% compared to 10 mM NaCl. In contrast, high ionic strength solutions imparted less effect on Ra adsorption to iron (hydr)oxides—Ra sorption to goethite and ferrihydrite in ASW only decreased 8 and 54 percent% compared to 10 mM NaCl, respectively. These results illustrate that clays possessing an exchangeable interlayer harbor appreciable Ra under low ionic strength conditions, but iron (hydr)oxides may control Ra sorption across shifting solution conditions such as those found within intertidal zones, etc. Nevertheless, all minerals experienced decreases in Ra sorption with increasing ionic strength, suggesting the increased presence of competing cations will reduce Ra sorption overall, even at trace levels. This is consistent with previous studies of Ra sorption in saline conditions, which also found similar results for iron (hydr)oxides.¹¹ However, it is important to note that some Ra is still retained by these surfaces even under high ionic strength conditions, suggesting that soil-sedimentary solids may serve as persistent sources or sinks of Ra despite large shifts in solution composition.

Figure 3. Impact of ionic strength on Ra sorption (mixed cation solutions, pH 7).



Author: Please examine Figure 3 to verify that the y-axis should read “Fraction Sorbed (.)”.

Surface Complexation Modeling

For ferrihydrite and goethite, fits of isotherm data to the SCM (see [Table 1](#) for Ra surface complexes considered and [SI](#) for the full set of reactions considered) produced good visual fits. When these isotherm-derived log K values were used to simulate experiments with different background cations, the fits were also reasonable (root mean squared error (RMSE) of Ra fraction sorbed over all conditions: 0.31 and 0.16 for ferrihydrite and goethite respectively). Fitting iron (hydr)oxide Ra log K values to the different background electrolyte experiments in aggregate resulted in improved fits to the background cation data (RMSE: 0.16 and 0.10) ([Table 1](#)), but produced worse visual fits for the isotherm data. While the fits are reasonable to each data set, the corresponding log K values for isotherm and background electrolyte derived log K s varied at least by 1 log unit, and often many more, suggesting the model fits have only limited predictive power when extended to natural background solutions and minerals.

Table 1. Ra SCM reactions, fitted log K values from isotherm and salinity varied experimental data, and RMSE for fits to variable background cation solutions.

Mineral	Reactions	$\log K$ Isotherm	K salinity RMSE	$\log K$ Salinity	K salinity RMSE
Ferrihydrite	$\text{tFhy}_s\text{OH} + \text{Ra}^{2+} \rightleftharpoons \text{tFhy}_s\text{OHRa}^{2+}$ $\text{Fhy}_s\text{OH} + \text{Ra}^{2+} \rightleftharpoons \text{Fhy}_s\text{OHRa}^{2+}$	6.7	0.31	5.7	0.16
	$\text{tFhy}_w\text{OH} + \text{Ra}^{2+} \rightleftharpoons \text{tFhy}_w\text{ORa}^{2+} + \text{H}^+$ $\text{Fhy}_w\text{OH} + \text{Ra}^{2+} \rightleftharpoons \text{Fhy}_w\text{ORa}^{2+} + \text{H}^+$	-2.8		-11.0	
	$\text{tFhy}_w\text{OH} + \text{Ra}^{2+} + \text{H}_2\text{O} \rightleftharpoons \text{tFhy}_w\text{ORaOH} + 2\text{H}^+$ $\text{Fhy}_w\text{OH} + \text{Ra}^{2+} + \text{H}_2\text{O} \rightleftharpoons \text{Fhy}_w\text{ORaOH} + 2\text{H}^+$	-15		-9.4	

Mineral	Reactions	$\log K$ Isotherm	Salinity RMSE	$\log K$ Salinity	Salinity RMSE
Goethite	$\text{tGoeOH} + \text{Ra}^{2+} \rightleftharpoons \text{tGoeORa}^+ + \text{H}^+$ $\text{tGoeOH} + \text{Ra}^{2+} \rightleftharpoons \text{GoeORa}^+ + \text{H}^+$ $\text{tGoeOH} + \text{Ra}^{2+} \rightleftharpoons \text{tGoeOHRa}^{2+} + \text{H}^+$ $\text{GoeOH} + \text{Ra}^{2+} \rightleftharpoons \text{GoeOHRa}^{2+}$	-3.9	0.16	-2.5	0.10
Sodium Montmorillonite	$\text{tClaysOH} + \text{Ra}^{2+} \rightleftharpoons \text{tClaysORa}^+ + \text{H}^+$ $\text{tClaysOH} + \text{Ra}^{2+} \rightleftharpoons \text{Clays} + \text{ORa}^+ + \text{H}^+$ $\text{tClay}_{\text{w1}}\text{OH} + \text{Ra}^{2+} \rightleftharpoons \text{tClay}_{\text{w1}}\text{ORa}^+ + \text{H}^+$ $\text{tClay}_{\text{w1}}\text{OH} + \text{Ra}^{2+} \rightleftharpoons \text{Clay}_{\text{w1}} + \text{ORa}^+ + \text{H}^+$ $2\text{tClay-Na} + \text{Ra}^{2+} \rightleftharpoons \text{tClay}_2\text{-Ra} + 2\text{Na}^+$ $\text{Clay-Na} + \text{Ra}^{2+} \rightleftharpoons \text{Clay}_2\text{-Ra} + 2\text{Na}^+$	0.0	0.38	-0.9	0.37
		-2.1		-1.9	
		0.2		0.2	

Surface complexation modeling of Ra sorption to montmorillonite was achieved through inclusion of an ~~inter-layer~~ interlayer exchange reaction, which was necessary to reproduce the high amount of Ra sorption observed at low pH values. Isotherm fitted $\log K$ values and background cation fitted $\log K$ values had poor background cation RMSEs and isotherm visual fits as compared to the iron (hydr)oxides (Table 1). Importantly, selectivity coefficients are only cautiously used to explain Ra interlayer exchange, as they are specifically derived for trace levels of competing cation.²³ Used as is, they will inaccurately predict competition between Ra and other competing cations, because they do not account for changes in the activity of clay exchange sites as the competing cation exchanges with Na in the clay ~~inter-layers~~ interlayers, explaining the poor fits observed. Removal of these selectivity coefficients from this model, however, resulted in overprediction of Ra sorption compared to experimental results and worse fits, since the models did not consider competitive exchange between Ra and the various background cations considered. Nevertheless, the necessary inclusion of an exchange reaction illustrates that Ra sorption to sodium montmorillonite is mechanistically distinct from other solids (e.g., iron (hydr)oxides), resulting in differential Ra sorption trends across solution conditions. 2:1 clay minerals may retain Ra under conditions where other minerals act as poor sorbents (e.g., low pH), but Ra sorption to those minerals is more prone to alteration when solution cation composition is varied. Implications for Ra mobility in soils, sediments, and aquifers

Results of this study provide context for sorption controls on Ra mobility within contaminated systems, and where Ra activities and isotopic ratios are used as hydrologic tracers. For example, handling and storage of large volumes of Ra-bearing wastewater produced during hydraulic fracturing operations pose a potential risk to soils, surface waters, and aquifers; accordingly, the use of Ra isotopes as markers for contamination associated with unconventional gas development has been examined, as the Ra isotopic ratios of the formation brines are typically different from shallow groundwater.^{38,39} Further, sorption represents a dominant control on Ra mobility within zones of subterranean groundwater discharge (SGD) from the land to the ocean.^{9,40-42} Few studies have examined detailed mineralogical

controls on sedimentary Ra sorption in SGD systems, but instead typically focus on general characteristics associated with sediment-Ra K_d value (e.g., particle size distribution, sand-silt-clay fraction).⁹ Accounting for specific mineral phases in SGD and other systems, including those which are redox-sensitive, may help constrain sources of variation. Radium retention is typically highest within soils, aquifer materials, and SGD sediments rich in Fe and Mn (hydr)oxides, such as those found within a subsurface “iron curtain”, found in Waquoit Bay, MA;⁴¹ as expected, our results mirror these observations, as goethite and ferrihydrite sorb appreciable quantities of Ra around circumneutral pH (FigFigure 1). Additionally, liberation of Ra to porewater is observed in SGD zones upon transition to reducing conditions, presumably through reductive dissolution of Ra-bearing Fe (and Mn) (hydr)oxides, including ferrihydrite, goethite, lepidocrocite, and hematite.^{41,43} Reducing conditions also favor the transformation of high-surface area metal (hydr)oxides, such as ferrihydrite, to those with greater thermodynamic stability, lower surface area, and consequently, less sorptive capacity per unit mass.^{14,44} Sorbed elements, such as U(VI), may be incorporated into secondary minerals during transformation.⁴⁵ However, Sajih et. al. measured no appreciable incorporation of sorbed Ra within secondary minerals during Fe²⁺ catalyzed conversion of ferrihydrite to goethite and magnetite.¹⁴ Hence, ripening of amorphous iron (hydr)oxides will result in Ra release to solution, supported here by less observed Ra sorption to goethite on a mass basis relative to ferrihydrite (FigFigure 1 a). Under sustained reducing conditions, metal sulfides and other reduced or mixed-valence iron (hydr)oxides form within sediments that are relevant to Ra contamination and SGD, such as mackinawite, pyrite, green rust(s), and magnetite. Of these, we examined Ra sorption to pyrite and found it to sorb most extensively compared to other minerals when normalized to surface area, which is somewhat surprising based on numerous studies that report Ra release and enhanced mobility under reducing conditions.^{41,43} However, despite extensive Ra sorption to pyrite relative to other minerals based on surface area (FigFigure 1 b), a substantial quantity of Ra remains in solution following equilibrium, and less Ra is retained by pyrite with increasing salinity (FigFigure 3). Hence, pyrite may sorb substantial Ra under low salinity conditions, but retain little Ra within saline natural waters including seawater and deep aquifer brines. Nevertheless, this unexpected result underscores the need for a better understanding of how Ra associates with minerals found under different redox conditions. For example, within reducing sediments, green rust (layered mixed-valence ferrie-ferric hydroxides) form and are capable of incorporating monovalent cations, and although less abundant than Fe (hydr)oxides, Mn (hydr)oxides are also present within zones of SGD and sorb Ra more extensively.⁴⁶ It is unknown whether Ra undergoes structural incorporation with these minerals, as observed for Cs⁺ association with sulfate green rust, or U(VI) incorporation into biogenic manganese oxides.⁴⁷ While redox controls on mineralogical composition clearly impart important controls on Ra mobility, 2:1 clay minerals persist across a range of conditions, and harbor appreciable quantities of Ra. Here, montmorillonite sorbed significant quantities of Ra, and may thereby represent a pool of sorbed radium that is (relatively) redox stable compared to metal (hydr)oxides. While not examined here, it is plausible that Ra associates with frayed edge sites within partially weathered primary clays, such as those found in Waquoit bay, similar to that observed for Cs⁺ sorption to micas within Hanford sediments.⁴⁸

In addition to co-precipitation (i.e., with barite), sorption is also an important process that controls Ra retention and release within host rock subjected to unconventional gas extraction. Aqueous Ra naturally accumulates within porewater associated with tight shales, and is mobilized to the surface with flowback and produced water following the injection of engineered fluids and subsequent natural gas recovery.^{49–51} While the injected fluid typically does not include Ra, produced waters include a formation brine component that often contains appreciable amounts of Ra (e.g., ~0.1–100 Bq/L in the Marcellus shale), having had long times to reach secular equilibrium with parent isotopes.^{51,52} Formation brines are extremely saline, often more so than seawater, thus aqueous Ra concentrations are expected to reflect the balance of Ra production and consumption by alpha recoil and radioactive decay. Accidental release, or permitted discharge of the produced water introduces this deep formation generated Ra to shallow aquifers and local watersheds, where the reduced ionic strength relative to the shale formation will drive enhanced Ra retention by shallow aquifer solids and surficial soils. Injection of engineered fluids could also enhance in-situ Ra sorption, perhaps transiently, owing to localized decreases in salinity, and oxidation of reduced Fe²⁺ minerals (e.g., siderite) to those capable of retaining high levels of Ra, including iron (hydr)oxides. Conversely, decreased sorption may occur through alteration of mineral surfaces such as pyrite, which retains the highest levels of Ra among all minerals examined here (FigFigure 1 b); however, this is only true when comparing Ra sorption normalized to surface area under low salinity conditions, highlighting that mineral surface area and competing ions within background solutions are critical factor governing extent of Ra sorption. Indeed, while Ra may sorb to these mineral surfaces in either scenario, the high ionic strength of natural shale formations would imply only a limited amount of Ra sorption overall. While it

is unclear whether alteration of mineral surfaces and geochemical conditions within shale formations will alter the in-situ mobility of Ra, results here and presented by others suggest that salinity and redox-perturbations will impart pronounced effects. The perturbations in Ra brine content induced by hydraulic fracturing operations will certainly influence the resultant Ra content of produced waters, thereby impacting the associated risks with handling and long-term fate of those produced waters. Better understanding of these geochemical impacts may allow operators to tune injected fluid chemistry to result in reduced Ra concentrations in produced water, helping to mitigate those risks.

These scenarios and the results here highlight that further work is needed to constrain how Ra sorption will influence the natural variability of Ra in the environment, as well as the mineral specific mechanisms that control Ra sorption. Here, the use of relatively simple SCMs has constrained possible mechanisms of sorption, but further study, including the role of competing cations on Ra sorption, is needed to improve modeling efforts, particularly in addressing competition between Ra and other sorbing cations. Further investigation of Ra interactions with key sedimentary minerals and mineral surfaces, including Mn (hydr)oxides, is also required to improve mechanistic descriptions used in modeling efforts, particularly those used for describing Ra transport within soil and sedimentary systems with fluctuating geochemical conditions driven by tidal activity, variable groundwater flow, and the industrial extraction and processing of Ra-bearing groundwater generated from hydraulic fracturing.

Acknowledgments. The authors thank Mitch Galanek, MIT Environmental Health and Safety, for supplying ^{226}Ra stock solutions, radiation protection equipment, and safety expertise, Neha Mehta (MIT) for her assistance with scintillation/gamma counting, Tiffany Wang (MIT) for assisting with isotherm experiments, and Dara Hok of the Kim Lab (Chapman University) for performing the BET analysis. This work was partially supported by the MIT energy initiative (MITEI). The authors declare no competing financial interest.

Supporting Information

Supporting Information

Additional descriptions The Supporting Information is available free of methods and results are charge on the ACS Publications website presented in supporting at DOI: [10.1021/acs.est.7b05443](https://doi.org/10.1021/acs.est.7b05443) information.

Additional descriptions of methods and results (PDF)

The authors declare no competing financial interest.

References

- (1) Zhang, T.; Gregory, K.; Hammack, R. W.; Vidic, R. D. Co-precipitation of radium with barium and strontium sulfate and its impact on the fate of radium during treatment of produced water from unconventional gas extraction. *Environ. Sci. Technol.* **2014**, *48* (8), 4596–4603 [10.1021/es405168b](https://doi.org/10.1021/es405168b).
- (2) Jones, A. P. Indoor air quality and health. *Atmos. Environ.* **1999**, *33* (28), 4535–4564 [10.1016/S1352-2310\(99\)00272-1](https://doi.org/10.1016/S1352-2310(99)00272-1).
- (3) Ivanovich, M. Uranium Series Disequilibrium - Concepts and Applications. *Radiochim. Acta* **1994**, *64* (2), 81–94 [10.1524/ract.1994.64.2.81](https://doi.org/10.1524/ract.1994.64.2.81).
- (4) Szabo, Z.; dePaul, V. T.; Fischer, J. M.; Kraemer, T. F.; Jacobsen, E. Occurrence and geochemistry of radium in water from principal drinking-water aquifer systems of the United States. *Appl. Geochemistry* **2012**, *27* (3), 729–752 [10.1016/j.apgeochem.2011.11.002](https://doi.org/10.1016/j.apgeochem.2011.11.002).
- (5) Barbot, E.; Vidic, N. S. N.; Gregory, K. B. K. B.; Vidic, R. D. R. Spatial and temporal correlation of water quality parameters of produced waters from Devonian-age shale following hydraulic fracturing. *Environ. Sci. Technol.* **2013**, *47* (6), 2562–2569 [10.1021/es304638h](https://doi.org/10.1021/es304638h).
- (6) Lauer, N. E.; Harkness, J. S.; Vengosh, A. Brine Spills Associated with Unconventional Oil Development in North Dakota. *Environ. Sci. Technol.* **2016**, *50* (10), 5389–5397 [10.1021/acs.est.5b06349](https://doi.org/10.1021/acs.est.5b06349).
- (7) Grivé, M.; Duro, L.; Colàs, E.; Giffaut, E. Thermodynamic data selection applied to radionuclides and chemotoxic elements: An overview of the ThermoChimie-TDB. *Appl. Geochemistry* **2015**, *55*, 85–94 [10.1016/j.apgeochem.2014.12.017](https://doi.org/10.1016/j.apgeochem.2014.12.017).
- (8) Fesenko, S.; Carvalho, F.; Martin, P.; Moore, W. S.; Yankovich, T. Radium in the Environment. *The Environmental Behavior of Radium: Revised Edition*. **2014**, 33–105.
- (9) Gonneea, M. E.; Morris, P. J.; Dulaiova, H.; Charette, M. a. New perspectives on radium behavior within a subterranean estuary. *Mar. Chem.* **2008**, *109* (3–4), 250–267 [10.1016/j.marchem.2007.12.002](https://doi.org/10.1016/j.marchem.2007.12.002).

- (10) Beneš, P.; Strejc, P.; Lukavec, Z.; Borovec, Z. Interaction of radium with freshwater sediments and their mineral components. I. *J. Radioanal. Nucl. Chem. Artic.* **1984**, *82* (2), 275–285 10.1007/BF02037050.
- (11) Ames, L.; McGarrah, J.; Walker, B. Sorption of trace constituents from aqueous solutions onto secondary minerals. II. Radium. *Clays Clay Miner.* **1983**, *31* (5), 335–342 10.1346/CCMN.1983.0310502.
- (12) Ames, L. L.; McGarrah, J. E.; Walker, B. A.; Salter, P. F. Uranium and radium sorption on amorphous ferric oxyhydroxide. *Chem. Geol.* **1983**, *40* (1–2), 135–148 10.1016/0009-2541(83)90095-5.
- (13) Koulouris, G. Sorption and distribution of Ra-226 in an electrolytic manganese dioxide column in the presence of other ions. *J. Radioanal. Nucl. Chem.* **1996**, *212* (2), 131–141 10.1007/BF02162345.
- (14) Sajih, M.; Bryan, N. D. D.; Livens, F. R. R.; Vaughan, D. J. J.; Descostes, M.; Phrommavanh, V.; Nos, J.; Morris, K. Adsorption of radium and barium on goethite and ferrihydrite: A kinetic and surface complexation modelling study. *Geochim. Cosmochim. Acta* **2014**, *146*, 150–163 10.1016/j.gca.2014.10.008.
- (15) Beck, A. J.; Cochran, M. a. Controls on solid-solution partitioning of radium in saturated marine sands. *Mar. Chem.* **2013**, *156*, 38–48 10.1016/j.marchem.2013.01.008.
- (16) Tamamura, S.; Takada, T.; Tomita, J.; Nagao, S.; Fukushima, K.; Yamamoto, M. Salinity dependence of 226Ra adsorption on montmorillonite and kaolinite. *J. Radioanal. Nucl. Chem.* **2013**, *299* (1), 569–575 10.1007/s10967-013-2740-3.
- (17) Schwertmann, U.; Cornell, R. *Iron Oxides in the Laboratory*; Wiley-VCH Verlag GmbH: Weinheim, Germany, 2000.
- (18) Jia, G.; Jia, J. Determination of radium isotopes in environmental samples by gamma spectrometry, liquid scintillation counting and alpha spectrometry: a review of analytical methodology. *J. Environ. Radioact.* **2012**, *106*, 98–119 10.1016/j.jenvrad.2011.12.003.
- (19) Parkhurst, D. L.; Appelo, C. A. J. Description of Input and Examples for PHREEQC Version 3 — SA Computer Program for Speciation, Batch-Reaction, One-Dimensional Transport, and Inverse Geochemical Calculations. *U.S. Geol. Surv. Tech. Methods* **2013**.
- (20) Python Software Foundation. Python Language Reference <https://www.python.org/>.
- (21) Dzombak, D.; Morel, F. *Surface Complexation Modeling: Hydrous Ferric Oxide*; Wiley: New York, NY, 1990.
- (22) Baeyens, B.; Bradbury, M. H. A mechanistic description of Ni and Zn sorption on na-montmorillonite. Part I: Titration and sorption measurements. *J. Contam. Hydrol.* **1997**, *27* (3–4), 199–222 10.1016/S0169-7722(97)00008-9.
- (23) Mathur, S. S.; Dzombak, D. A. Surface-complexation modeling. In *Surface complexation modeling*; Lutzenkirchen, J., Ed.; 2006; pp 443–468.
- (24) van Geen, A.; Robertson, A. P.; Leckie, J. O. Complexation of carbonate species at the goethite surface: Implications for adsorption of metal ions in natural waters. *Geochim. Cosmochim. Acta* **1994**, *58* (9), 2073–2086 10.1016/0016-7037(94)90286-0.
- (25) The Clay Minerals Society. Source Clay Physical/Chemical Data http://clays.org/sourceclays_data.html (accessed Dec 10, 2017).
- (26) Tournassat, C.; Ferrage, E.; Poinssignon, C.; Charlet, L. The titration of clay minerals: II. Structure-based model and implications for clay reactivity. *J. Colloid Interface Sci.* **2004**, *273* (1), 234–246 10.1016/j.jcis.2003.11.022.
- (27) Charlet, L.; Tournassat, C. Fe(II)-Na(I)-Ca(II) cation exchange on montmorillonite in chloride medium: Evidence for preferential clay adsorption of chloride - Metal ion pairs in seawater. *Aquat. Geochemistry* **2005**, *11* (2), 115–137 10.1007/s10498-004-1166-5.
- (28) Bradbury, M. H.; Baeyens, B. A mechanistic description of Ni and Zn sorption on Part II: modelling. *J. Contam. Hydrol.* **1997**, *27*, 223–248 10.1016/S0169-7722(97)00008-9.
- (29) Bradbury, M. H.; Baeyens, B. Modelling the sorption of Mn(II), Co(II), Ni(II), Zn(II), Cd(II), Eu(III), Am(III), Sn(IV), Th(IV), Np(V) and U(VI) on montmorillonite: Linear free energy relationships and estimates of surface binding constants for some selected heavy metals and actinide. *Geochim. Cosmochim. Acta* **2005**, *69* (4), 875–892 10.1016/j.gca.2004.07.020.
- (30) Michel, F. M.; Ehm, L.; Antao, S. M.; Lee, P. L.; Chupas, P. J.; Liu, G.; Strongin, D. R.; Schoonen, M. A. A.; Phillips, B. L.; Parise, J. B. The structure of ferrihydrite, a nanocrystalline material. *Science* **2007**, *316* (5832), 1726–1729 10.1126/science.1142525.
- (31) Cornell, R. M.; Schwertmann, U. Crystal structure. In *The Iron Oxides: Structure, Properties, Reactions, Occurrences and Uses*; Wiley-VCH Verlag GmbH: Weinheim, 2003; pp 9–38.

- (32) Naveau, A.; Monteil-Rivera, F.; Dumonceau, J.; Catalette, H.; Simoni, E. Sorption of Sr(II) and Eu(III) onto pyrite under different redox potential conditions. *J. Colloid Interface Sci.* **2006**, *293* (1), 27–35.10.1016/j.jcis.2005.06.049.
- (33) Murphy, R.; Strongin, D. Surface reactivity of pyrite and related sulfides. *Surf. Sci. Rep.* **2009**, *64* (1), 1–45.10.1016/j.surfrep.2008.09.002.
- (34) Kornicker, W. A.; Morse, J. W. Interactions of divalent cations with the surface of pyrite. *Geochim. Cosmochim. Acta* **1991**, *55* (8), 2159–2171.10.1016/0016-7037(91)90094-L.
- (35) Wersin, P.; Hochella, M. F.; Persson, P.; Redden, G.; Leckie, J. O.; Harris, D. W. Interaction between aqueous uranium (VI) and sulfide minerals: Spectroscopic evidence for sorption and reduction. *Geochim. Cosmochim. Acta* **1994**, *58* (13), 2829–2843.10.1016/0016-7037(94)90117-1.
- (36) Naveau, A.; Monteil-Rivera, F.; Guillon, E.; Dumonceau, J. Interactions of aqueous selenium (-II) and (IV) with metallic sulfide surfaces. *Environ. Sci. Technol.* **2007**, *41* (15), 5376–5382.10.1021/es0704481.
- (37) Das, D. K.; Pathak, P. N.; Kumar, S.; Manchanda, V. K. Sorption behavior of Am³⁺ on suspended pyrite. *J. Radioanal. Nucl. Chem.* **2009**, *281* (3), 449–455.10.1007/s10967-009-0030-x.
- (38) Warner, N. R.; Kresse, T. M.; Hays, P. D.; Down, A.; Karr, J. D.; Jackson, R. B.; Vengosh, A. Geochemical and isotopic variations in shallow groundwater in areas of the Fayetteville Shale development, north-central Arkansas. *Appl. Geochemistry/Geochem.* **2013**, *35*, 207–220.10.1016/j.apgeochem.2013.04.013.
- (39) Lauer, N.; Vengosh, A. Age Dating Oil and Gas Wastewater Spills Using Radium Isotopes and Their Decay Products in Impacted Soil and Sediment. *Environ. Sci. Technol. Lett.* **2016**, *3* (5), 205–209.10.1021/acs.estlett.6b00118.
- (40) Hughes, A. L. H.; Wilson, A. M.; Moore, W. S. Groundwater transport and radium variability in coastal porewaters. *Estuar. Coast. Estuarine, Coastal Shelf Sci.* **2015**, *164*, 94–104.10.1016/j.ecss.2015.06.005.
- (41) Gonneea, M. E.; Mulligan, A. E.; Charette, M. A. Seasonal cycles in radium and barium within a subterranean estuary: Implications for groundwater derived chemical fluxes to surface waters. *Geochim. Cosmochim. Acta* **2013**, *119*, 164–177.10.1016/j.gca.2013.05.034.
- (42) Burnett, B.; Chanton, J.; Christoff, J.; Kontar, E.; Krupa, S.; Lambert, M.; Moore, W.; O'Rourke, D.; Paulsen, R.; Smith, C. et al. Assessing methodologies for measuring groundwater discharge to the ocean. *Eos, Trans. Am. Geophys. Union* **2002**, *83* (11), 117.10.1029/2002EO000069.
- (43) Charette, M. a.; Sholkovitz, E. R.; Hansel, C. M. Trace element cycling in a subterranean estuary: Part 1. Geochemistry of the permeable sediments. *Geochim. Cosmochim. Acta* **2005**, *69* (8), 2095–2109.10.1016/j.gca.2004.10.024.
- (44) Hansel, C. M.; Wielinga, B. W.; Fendorf, S. Structural and compositional evolution of Cr/Fe solids after indirect chromate reduction by dissimilatory iron-reducing bacteria. *Geochim. Cosmochim. Acta* **2003**, *67* (3), 401–412.10.1016/S0016-7037(02)01081-5.
- (45) Nico, P. S.; Stewart, B. D.; Fendorf, S. Incorporation of oxidized uranium into Fe (Hydr)oxides during Fe(II) catalyzed remineralization. *Environ. Sci. Technol.* **2009**, *43* (19), 7391–7396.10.1021/es900515q.
- (46) Christiansen, B. C.; Dideriksen, K.; Katz, A.; Nedel, S.; Bovet, N.; Sørensen, H. O.; Frandsen, C.; Gundlach, C.; Andersson, M. P.; Stipp, S. L. S. Incorporation of monovalent cations in sulfate green rust. *Inorg. Chem.* **2014**, *53* (17), 8887–8894.10.1021/ic500495a.
- (47) Webb, S. M.; Fuller, C. C.; Tebo, B. M.; Bargar, J. R. Determination of uranyl incorporation into biogenic manganese oxides using X-ray absorption spectroscopy and scattering. *Environ. Sci. Technol.* **2006**, *40* (3), 771–777.10.1021/es051679f.
- (48) Zachara, J. M.; Smith, S. C.; Liu, C.; McKinley, J. P.; Serne, R. J.; Gassman, P. L.; Acharya, J. O. H. N. M. Z.; Mith, S. T. C. S.; Iu, C. H. L.; Inley, J. A. P. M. C. K. et al. Sorption of Cs⁺ to micaceous subsurface sediments from the Hanford site, USA. *Geochim. Cosmochim. Acta* **2002**, *66* (2), 193–211.10.1016/S0016-7037(01)00759-1.
- (49) Kondash, A. J.; Warner, N. R.; Lahav, O.; Vengosh, A. Radium and barium removal through blending hydraulic fracturing fluids with acid mine drainage. *Environ. Sci. Technol.* **2014**, *48* (2), 1334–1342.10.1021/es403852h.
- (50) Vengosh, A.; Jackson, R. B.; Warner, N.; Darrah, T. H.; Kondash, A. A Critical Review of the Risks to Water Resources from Unconventional Shale Gas Development and Hydraulic Fracturing in the United States. *Environ. Sci. Technol.* **2014**, *48* (15), 8334–8348.10.1021/es405118y.
- (51) Rowan, E. L. ; Engle, M. A. ; Kirby, C. S. ; Kraemer, T. F. *Radium Content of Oil- and Gas-Field Produced Waters in the Northern Appalachian Basin (USA)* **2011**.

(52) Warner, N. R.; Christie, C. a.; Jackson, R. B.; Vengosh, A. Impacts of shale gas wastewater disposal on water quality in Western Pennsylvania. *Environ. Sci. Technol.* **2013**, *47*, 11849–1185710.1021/es402165b.